frontiers | Frontiers in Earth Science

TYPE Original Research
PUBLISHED 17 February 2023
DOI 10.3389/feart.2022.1021953

OPEN ACCESS

EDITED BY
Shangfeng Chen,
Institute of Atmospheric Physics (CAS), China

REVIEWED BY
Ping Liang,
Shanghai Meteorological Bureau, China
Lei Song,
Institute of Atmospheric Physics (CAS), China

*CORRESPONDENCE
Xiong Chen,
chenxmails@163.com

SPECIALTY SECTION
This article was submitted to Atmospheric Science, a section of the journal Frontiers in Earth Science

RECEIVED 18 August 2022
ACCEPTED 19 December 2022
PUBLISHED 17 February 2023

CITATION
Li L, Chen X, Li C, Li X and Yang M (2023), Comparison of Madden-Julian oscillation in three super El Niño events.
Front. Earth Sci. 10:1021953.
doi: 10.3389/feart.2022.1021953

Comparison of Madden-Julian oscillation in three super El Niño events

Lifeng Li[1], Xiong Chen[2]*, Chongyin Li[2,3], Xin Li[2] and Minghao Yang[2]

[1]Institute of Aerospace Information, Space Engineering University, Beijing, China, [2]College of Meteorology and Oceanography, National University of Defense Technology, Changsha, China, [3]State Key Laboratory of Numerical Modeling for Atmospheric Sciences and Geophysical Fluid Dynamics (LASG), Institute of Atmospheric Physics, Chinese Academy of Sciences, Beijing, China

This paper investigated the characteristics of Madden-Julian Oscillation (MJO) in three super El Niño events (i.e., 1982/83, 1997/98 and 2015/16 El Niño events) based on reanalysis data. MJO with apparent eastward propagation can be observed during the developing stages of these three super El Niño events. Enhanced MJO zonal wind was observed over the western Pacific, especially in 1997/98 and 2015/16 El Niño events, which is mainly attributed to the effects of tropical background circulation and extratropical anomalous circulation. During the mature stages of 1982/83 and 1997/98 El Niño events, MJO with noticeable eastward propagation cannot be observed, and the MJO zonal wind amplitude at 850 hPa was weakened (enhanced) over the Indian Ocean and western Pacific (central and eastern Pacific). However, MJO zonal wind amplitude over the central and eastern Pacific was enhanced and the prominent eastward propagation was also found in the mature stage of 2015/16 El Niño. The eastward propagation of MJO was also observed during the decaying stages of the three super El Niño events, but its intensity was weaker compared with the developing and mature stages. The abnormal activity of MJO during the mature and decaying stages may be closely related to the characteristics in circulation and moisture anomalies caused by El Niño and the seasonal cycle of circulation and moisture. In addition, this study found that the RMM index and MJO zonal wind amplitude may lead to contradictory results in identifying the characteristics of MJO activity, especially during the developing and decaying stages.

KEYWORDS

Madden-Julian Oscillation (MJO), super El Niño, comparative study, extratropical anomalous circulation, RMM index

1 Introduction

Madden-Julian Oscillation (MJO) is the most important component of tropical atmospheric intraseasonal oscillation (Madden and Julian, 1971; Madden and Julian, 1972), and is also the bridge between weather and climate, which means that MJO plays a critical role in the anomalous weather and climate in many regions (Zhang, 2013; Li et al., 2014; Li et al., 2020). El Niño–Southern Oscillation (ENSO), as the strongest signal of large-scale sea-air interaction, shows significant variability on interannual timescales in the tropical ocean and atmosphere. ENSO and MJO are two of the vital systems in the tropic. Although the time scales of ENSO and MJO are very different, they are closely related. The MJO plays an important role in the initiation and termination of ENSO (Lau and Chan, 1988; Takayabu et al., 1999; Bergman et al., 2001; Miyakawa et al., 2017). On the one hand, the strengthened MJO could induce a stronger stochastic forcing like westerly wind burst, which trigger the El Niño (Lau and Chan

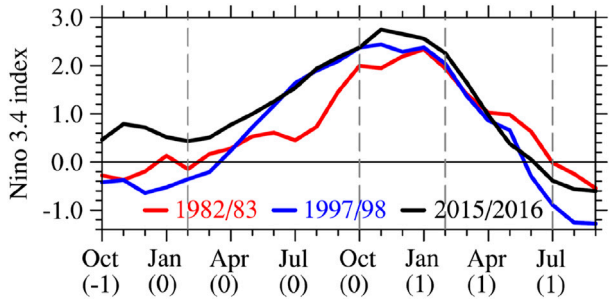

FIGURE 1
Evolution of monthly Niño 3.4 index during the three super El Niño events. The –1, 0 and 1 represent super El Niño event previous, onset and next year, respectively.

1988; Bergman et al., 2001). On the other hand, the robust MJO activities and its eastward propagation in May 1998 strengthened the easterly anomalies over the eastern Pacific, which caused the abrupt decaying of El Niño (Takayabu et al., 1999; Miyakawa et al., 2017). The MJO activity could be modulated by the ENSO (Lau and Chan, 1986; Moon et al., 2011; Lee et al., 2019; Wei and Ren, 2019). The El Niño might reduce the frequency of the MJO *via* the air–sea interactions (Lau and Chan, 1986). Wei and Ren (2019) indicated that ENSO can regulate the propagation of MJO. The equatorially symmetric eastward propagation of MJO is fast from the Indian Ocean to the equatorial western Pacific during El Niño, whereas the MJO during La Niña is very slow *via* the southern Maritime Continent. In addition, the teleconnection from the MJO could be modulated by the ENSO (Moon et al., 2011; Lee et al., 2019).

Accompany the evolution of El Niño, anomalous MJO activity can be observed in many regions (Li and Zhou, 1994; Hendon et al., 2007; Chen et al., 2015; Chen et al., 2016). MJO activity is enhanced over the western Pacific before the occurrence of El Niño, while it is weakened rapidly after El Niño (Li and Zhou, 1994; Li and Li, 1995). During the developing stages of El Niño, anomalous MJO activity will lead to westerly wind bursts in the western Pacific (Vecchi and Harrison, 2000; Hendon et al., 2007), causing sinking Kelvin wave in the ocean (Kessler et al., 1995; Seo and Xue, 2005), thus affecting the sea surface temperature in the equatorial Pacific and providing advantageous environment for the developing stages of El Niño (Zhang and Gottschalck, 2002; McPhaden et al., 2006). The combination of the atmospheric barotropic instable mode mainly excited by El Niño and the MJO circulation results in the MJO tending to a barotropic structure in the vertical direction during El Niño (Li and Li, 1995; Li and Smith, 1995; Chen et al., 2015). During the El Niño event, due to the increase of moisture and moist static energy over the central and eastern Pacific, MJO zonal winds in the lower tropospheric are enhanced over the central Pacific while it weakened over the western Pacific. Meanwhile, the location of the maximum growth rate of MJO moves eastward and the eastward propagation speed of the MJO slow down (Fink and Speth, 1997; Tam and Lau, 2005). In addition, the convective activity strengthens in the central and eastern Pacific during El Niño, changing the position of atmospheric adiabatic heating, so that the eastward propagation of the MJO is not obvious, and some regions have westward propagation, especially in the Pacific (Li, 1995; Li and Smith, 1995; Chen et al., 2015).

In recent years, many researchers have paid more attention to the relationship between the MJO and two types of El Niño, especially the relationship between the MJO and the central Pacific El Niño (Feng et al., 2015; Yuan et al., 2015). In the eastern Pacific El Niño, the MJO activity over the western Pacific are enhanced during spring and summer, while they are significantly weakened during the four to 5 months the after eastern Pacific El Niño matures (Gushchina and Dewitte, 2012; Chen et al., 2016). However, the enhancement of the MJO in the central Pacific El Niño mainly occur in the mature and decaying stages of El Niño (Gushchina and Dewitte, 2012; Chen et al., 2016). During the central Pacific El Niño, the anomalous circulation and moisture over the maritime continent and western Pacific are conductive to the increase of moist static energy and the conversion from barotropic and baroclinic energy from the low-frequency background field to MJO scale, thus strengthening the MJO activity in these regions (Hsu et al., 2018; Wang et al., 2018). The horizontal and vertical moisture advection over the central Pacific is stronger during the central Pacific El Niño compared with during the eastern Pacific El Niño, resulting in the stronger intensity and the furtherer eastward propagation of the MJO during the central Pacific El Niño (Chen et al., 2016). Dasgupta et al. (2021) indicated that the first and second MJO frequency pattern is most prominent during the negative central Pacific and positive eastern Pacific ENSO phases, respectively, which is caused by the horizontal convergence of mean background moisture through intraseasonal winds during the two types of ENSO phases.

This study selected three El Niño events (1982/83, 1997/98 and 2015/16 El Niño) with the strongest SST anomalies in recent decades, which are usually called super El Niño (Chen et al., 2016; Yuan et al., 2016; Mu and Ren, 2017; Abellán et al., 2018). The evolution characteristics of SST during the super El Niño and their effects on global weather and climate are significantly distinct compared with those during the ordinary El Niño (Li and Min, 2016; Bi et al., 2017; Liu et al., 2018; Qian and Guan, 2018). Affected by the 2015/16 El Niño event the precipitation significantly increased in the southern China during the autumn and winter in 2015, especially in the South China in winter, with the precipitation reaching the strongest value in history record (Yuan et al., 2016; Zhai et al., 2016). At the same time, there are many similarities and differences between the three super El Niño events (Shao and Zhou, 2016; Paek et al., 2017; Rao and Ren, 2017; Abellán et al., 2018). The center of positive SST anomaly during the 2015/16 El Niño was apparently westward compared with the previous two El Niño (Ren et al., 2017), which is the mixed characteristics of the central Pacific El Niño and eastern Pacific El Niño (Paek et al., 2017). The intraseasonal zonal westerly in the 2015/16 El Niño was weaker than that in the 1997/98 El Niño, which lead to weaker intraseasonal SST (Lyu et al., 2018). The thermocline feedback in the 2015/16 El Niño was weaker than the other two super El Niño, while the advection feedback was significantly enhanced (Zheng et al., 2019).

The super El Niño events have gradually received more attention due to the characteristics in the evolution and their enormous influence on the global weather and climate, which bring the new challenges to our research and forecasting. MJO and ENSO are the two systems with the most significant variation in the tropical atmosphere and ocean, and their interaction has always been a hot topic. The MJO activity appear significantly abnormal along with the evolution of El Niño. So what are the characteristics of MJO activity during super El Niño? What are the differences in MJO activities between the three super El Niño? In view of these problem, this paper will attempt to compare and analyze the abnormal characteristics of MJO from the

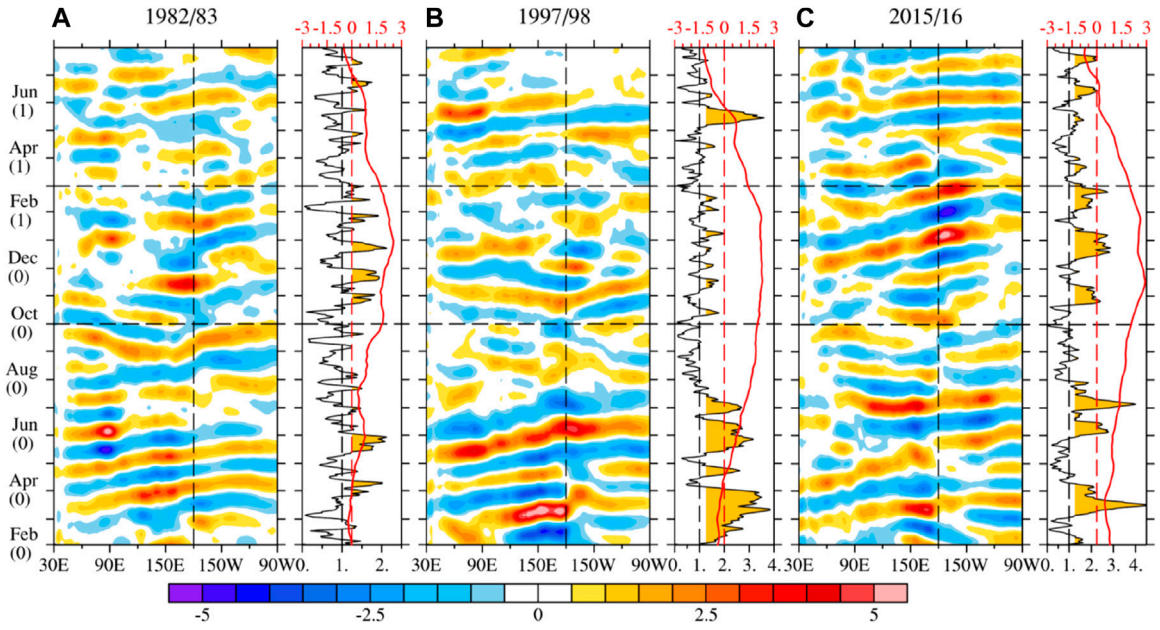

FIGURE 2
Evolution of MJO zonal wind at 850 hPa averaged over 10°S-10°N (colors shading, m s^{-1}), RMM index (black lines, RMM index exceeding 1.2 are marked with orange), and Niño 3.4 index (red lines) during three super El Niño events. The 0 and 1 represent super El Niño event onset and next year, respectively. **(A–C)** represent 1982/83,1997/98 and 2015/16, respectively.

developing, mature and decaying stages of the super El Nino events, and explore the relationship between MJO and super ENSO, so as to provide important support for the prediction of MJO. The paper is organized as follows. Section 2 describes the data and analysis techniques. The evolution characteristics of MJO and possible causes of anomalous MJO activity are presented in section 3 and section 4, respectively. We present concluding remarks with discussions in section 5.

2 Materials and methods

Daily mean atmospheric data at a horizontal resolution of 1.5 × 1.5, including horizontal winds and specific humidity, were from the European Center for Medium-Range Weather Forecasts Interim Re-Analysis (ERA-Interim; Dee et al., 2011). SST data were obtained from the National Oceanic and Atmospheric Administration (NOAA) for both temporal resolutions of daily (Optimum Interpolation SST V2; Reynolds et al., 2007) and monthly (Extended Reconstructed SST V5 (Huang et al., 2017), at a horizontal resolution of .25 × .25 and 2.0 × 2.0, respectively. Furthermore, daily real-time multivariate MJO indexes (RMM; Wheeler and Hendon, 2004) were obtained from the Australian Bureau of Meteorology, which is the multivariate combined EOF of 850 h Pa zonal wind, 200 h Pa zonal wind and outgoing longwave radiation. RMM can reflect the real-time variation of intensity and position for the MJO. The record length of all data compiled in this study is 39 years from 1 January 1979 to 31 December 2017.

Anomalies were obtained by removing the seasonal cycle and linear trend. The MJO signal was obtained by the Lanczos band-pass filter with 201 days of smoothing (Duchon, 1979). The time-space spectrum analysis is used to analyze the distribution of vibration energy with wave number and frequency (Hayashi, 1982). The evolution of the three super El Niño was represented by the Niño 3.4 index (SST anomaly average over the 5°S-5°N,170°-120°W). Figure 1 shows the evolution of the Niño 3.4 index during the three super El Niño. The maximum of Niño 3.4 index is higher than 2.0°C in super El Niño, while there are prominent differences in the evolution of Niño 3.4 index among the three events. According to the evolution of Niño 3.4 index, the super El Niño events can be divided into three stages: developing stages (from February to September) that is a stable growth period before Niño 3.4 index reaches 2.0°C, mature stages (from October to February of the following year) that is a period when Niño 3.4 index remains around 2.0°C, and decaying stages (from March of the following year to July) that is a period when Niño 3.4 index is below 2.0°C and turn into a negative value. The Niño 3.4 index turn from a negative anomaly to a positive anomaly except for the 2015/16 El Niño, which is mainly attributed to the warming events of the Pacific in 2014 (Zhai et al., 2016; Chen et al., 2017). In the decaying stages, the evolution of the Niño 3.4 index in the three super El Niño shows a similar pattern. However, the Niño 3.4 indices during developing stages are distinct, and it is prominent that the intensity of the Niño 3.4 index for the 1982/83 El Niño is significantly weaker compared with those for the other two El Niño events.

3 Activity and evolution of MJO

Figure 2 exhibits the evolution of MJO zonal wind at 850 hPa averaged over the 10°S-10°N, RMM index and Niño 3.4 index during the three super El Niño. It is evident that there are significant

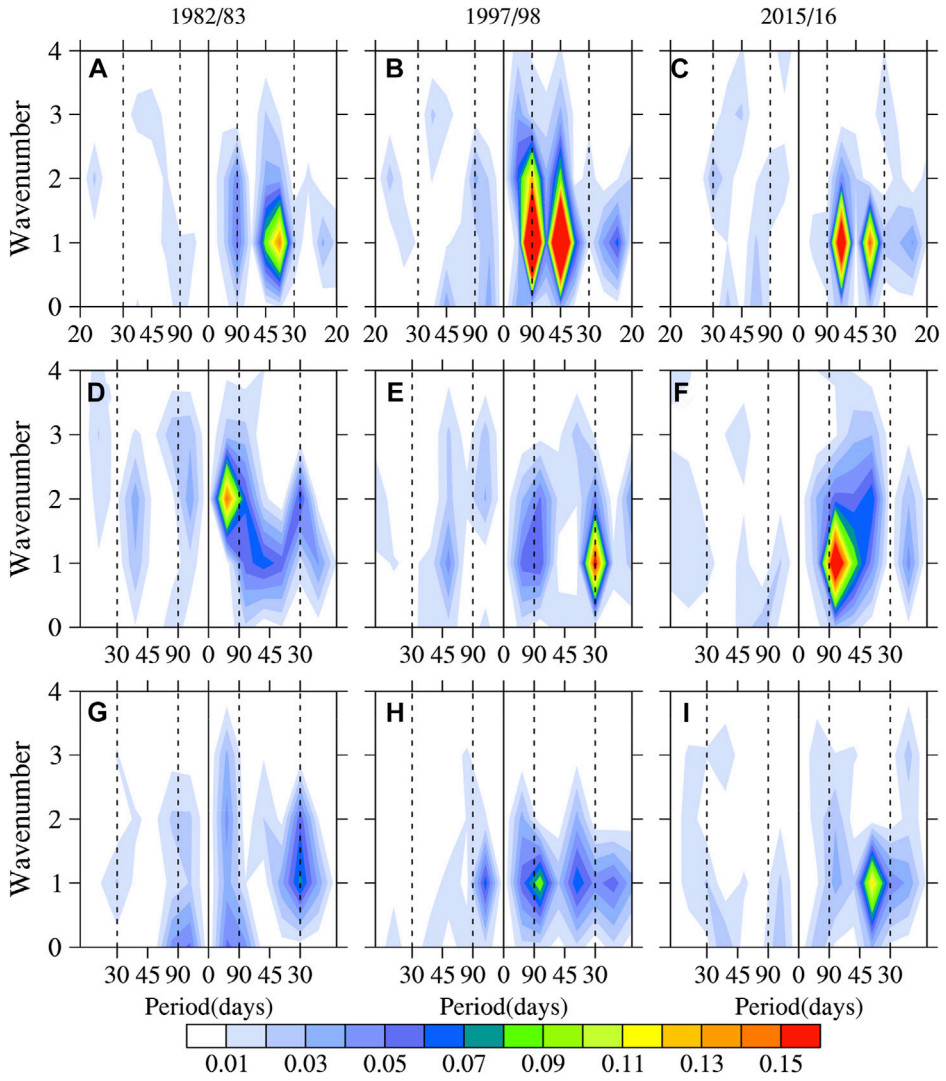

FIGURE 3
Time-space spectra of zonal wind at 850 hPa averaged over 10°S-10°N for 1982/83 (left), 1997/98 (middle), and 2015/16 (right) super El Niño during developing stages **(A–C)**, mature stages **(D–F)**, and decaying stages **(G–I)**.

discrepancies in the characteristics of MJO activity during the different stages in the three super El Niño.

3.1 Developing stage

In the developing stage, especially from February to July, the enhanced MJO significantly propagated eastward from the Indian Ocean to the Pacific during the three super El Niño (Figure 2). However, there were prominent differences in intensity, speed and distance of propagation. The spatiotemporal spectrum analysis (Figure 3) illustrated that the strongest power spectrum of eastward propagation occurs in the developing stages of 1997/98 El Niño with the main periods of 45 days and 90 days. During the 2015/16 El Niño, the power spectrum of eastward propagation was relatively weak with a major period of 40 days and 60 days. During the 1982/83 El Niño, the power spectrum of eastward propagation was the weakest with a main period of about 40 days. The eastward propagation of the MJO was primarily dominated by zonal 1 wave, and the eastward propagation of zonal 2 wave was also strong during the 1997/98 El Niño. In addition, eastward propagation of strong high-frequency waves with a period of about 25 days occurred during the developing stage, especially for 1997/98 El Niño.

The evolution of RMM index (Figure 2) illustrated that the strongest RMM index appeared in March 2015, and this robust MJO activity directly promoted the development of 2015/16 El Niño (Chen et al., 2017; Hong et al., 2017). The average value of RMM index is about 1.2 in winter. Thus, the strong MJO event is defined, when the RMM index is equal or greater than 1.2. The strong MJO event occurred with the longest duration in the developing stages of the 1997/1998 El Niño, while the relatively weak RMM index in the developing stages of the 1982/83 El Niño. Figure 4 depicts the evolution characteristics of MJO phase and intensity. Two strong MJO events occurred in the 1997/98 and 2015/16 El Niño events. Furthermore, the abnormal enhanced MJO activity primarily appeared in phase 5–8. However, the strengthened MJO activity mainly appeared in phase 1–3 during the

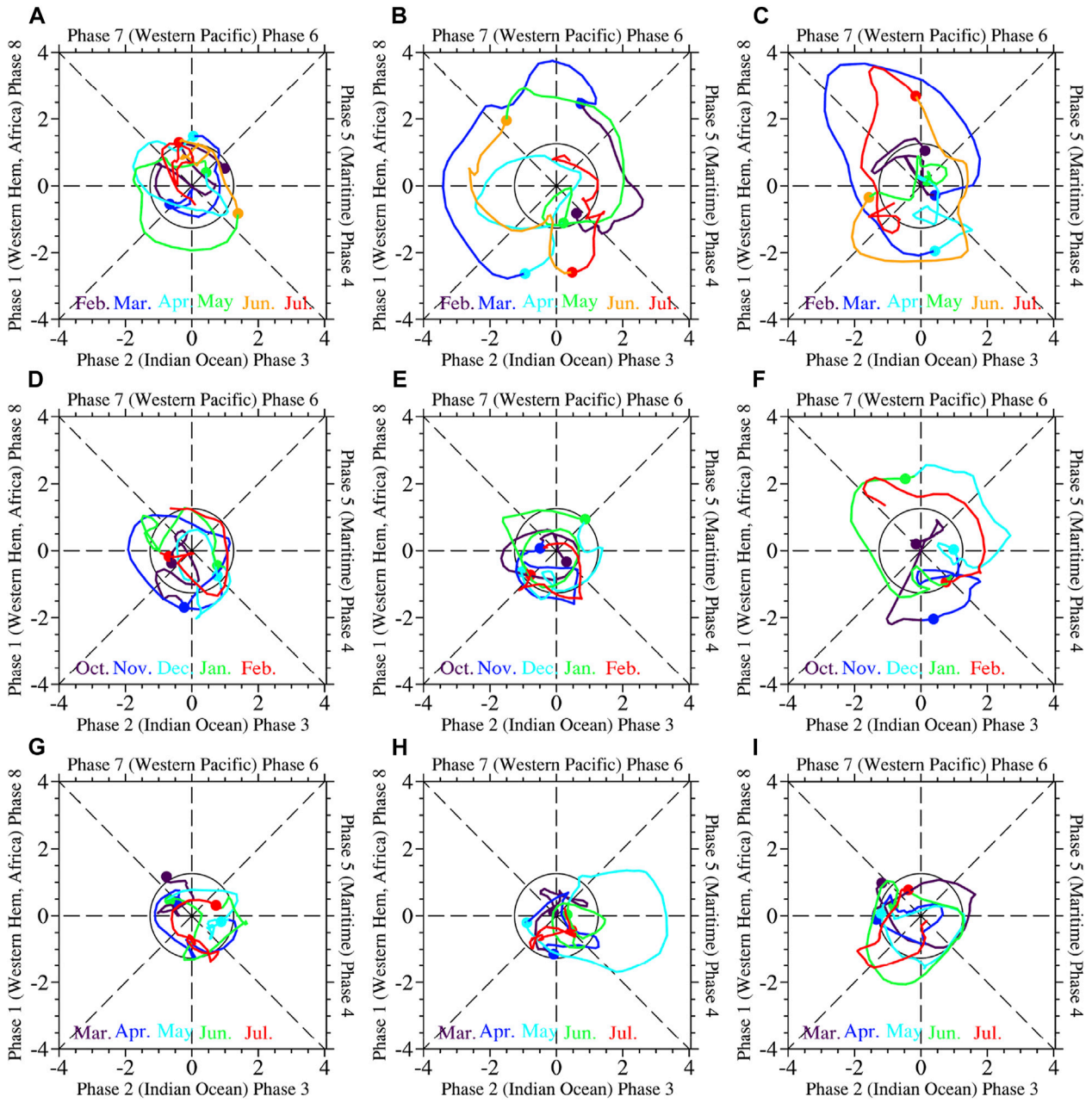

FIGURE 4
RMM index for 1982/83 (left), 1997/98 (middle), and 2015/16 (right) super El Niño during developing stages **(A–C)**, mature stages **(D–F)**, and decaying stages **(G–I)**.

developing stages of the 1982/83 El Niño. Many studies have shown that eastward propagation of the MJO zonal westerly during the 1997/98 El Niño and 2015/16 El Niño directly leads to the variation of ocean thermocline, thus promoting the development of El Niño (McPhaden, 1999; L'Heureux et al., 2017). As shown in Figure 2, two prominent eastward propagation of MJO zonal westerly appeared during the developing stages of the 1982/83 El Niño, and the MJO activity over the western Pacific were strengthened to a certain extent. However, the role of the MJO in the development of this El Niño event had not been deeply examined due to the lack of data. At the same time, weak MJO activities were detected during the developing stages of three super El Niño, particularly in the 1982/83 El Niño. The composite RMM index of each phase during the developing stages of three super El Niño showed that, on average, MJO activities in each phase weakened during the developing stages of the 1982/83 El Niño while enhanced in each phase during the 1997/98 El Niño, especially phase 1 and phase5-8. However, the MJO activities weakened in phase4-6 of the 2015/16 El Niño while strengthened in the other phases.

Some studies (Li and Li, 1995; Chen et al., 2015) suggest that MJO activities are significantly enhanced during the developing stages of the 1982/83 El Niño, whereas the composite RMM index shows that MJO activities are weakened during the developing stages of the 1982/83 El Niño, which may be related to the method used. Figure 6 exhibits the MJO zonal wind amplitude anomalies during the three super El Niño

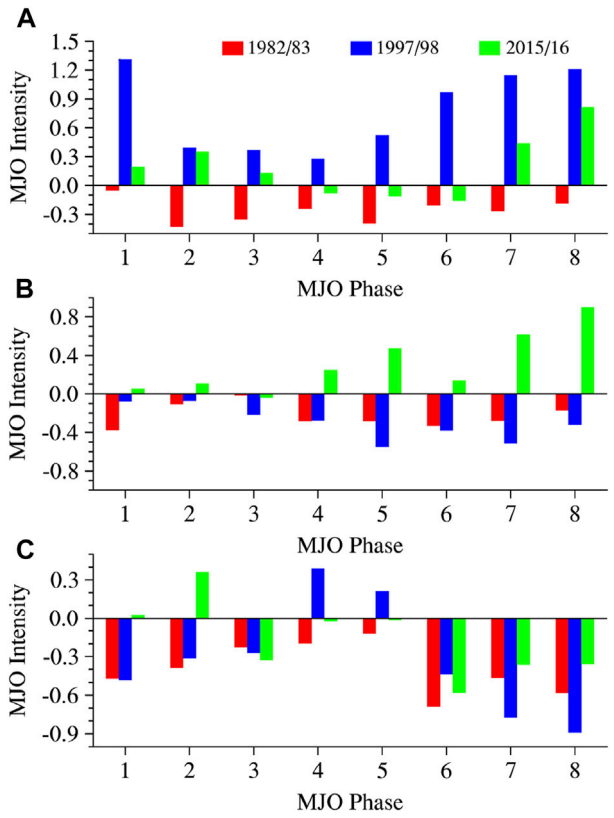

FIGURE 5
Composite RMM index at different MJO phases during the **(A)** developing stages, **(B)** mature stages, and **(C)** decaying stages for the three super El Niño events.

events. The MJO zonal wind amplitude refers to the 3-month sliding standard deviation of MJO zonal wind at 850 hPa (Chen et al., 2016). It was clear that MJO zonal wind amplitude in the developing stages of the three El Niño events were strengthened, but there were also obvious differences. The positive MJO amplitude anomalies were the weakest and primarily concentrated in the western Pacific during the developing stages of the 1982/83 El Niño. The MJO over the Indian Ocean near 90°E was also enhanced from April to July. For the 1997/98 El Niño, the MJO amplitude anomalies were the strongest, and they are significantly strengthened throughout the Indian Ocean and Pacific in the spring and early summer. The abnormal intensity of MJO amplitude in the 2015/16 El Niño was between the previous El Niño events, and the enhanced MJO amplitude mainly occurred in the Pacific, while there were negative MJO amplitude anomalies in the Indian Ocean. These results indicate that there are certain differences between the anomalous MJO zonal amplitude and anomalous RMM index. The discrepancies may be attributed to the differences in the analysis methods and emphases that evaluate the MJO intensity, which leads to contradictory results in different studies.

3.2 Mature stages

During the mature stages of the 2015/16 El Niño, the robust MJO was detected along with significant eastward propagation over the Indian Ocean and Pacific. In contrast, the MJO activities were weakened during the other two super El Niño, and their eastward propagation were not prominent, and even westward propagation existed in some regions (Figure 2). The spatiotemporal spectral analysis as shown in Figure 3 illustrated that the power spectrum of eastward propagation in the intraseasonal scale was the strongest during the mature stages of the 2015/16 El Niño, with a central period of about 75 days, whereas they were significantly weakened during the 1982/83 El Niño and 1997/98 El Niño, especially in the 1997/98 El Niño. The intraseasonal wave of eastward propagation was primarily zonal wave 1, while the zonal wave 2 was also robust during the 2015/16 El Niño. The prominently enhanced eastward propagation of zonal wave 2 of more than 90 days appeared in the mature stages of the 1982/83 El Niño, which may be caused by the conversion of the MJO energy to low-frequency energy of more than 90 days (Li and Zhou, 1994; Li and Li, 1995). In addition, the power spectrum of westward propagation at the intraseasonal and low-frequency (>90 days) scales were also significantly enhanced during the 1982/83 and 1997/98 El Niño events.

MJO intensity weakened during the mature stages compared with that during the developing stages, especially in the 1997/98 El Niño (Figure 4), which is consistent with previous studies that the MJO activity is enhanced during the developing stages of El Niño, while weakened during the mature stages (Li and Zhou, 1994; Li and Li, 1995). During the mature stages of the 1982/83 El Niño, RMM indexes of some days were stronger than the climate mean. The prominent MJO activity were not observed during the mature stages of the 1997/98 El Niño. However, two significant eastward propagation appeared in the 2015/16 El Niño, and the enhanced MJO activities were primarily located in phase 5–8. The composite RMM index of different phase (Figure 5) showed that MJO activities were weakened during the mature stages of the 1982/83 and 1997/98 El Niño events, especially at phase 4–8. However, the MJO activities were enhanced except for phase 3 during the mature stages of the 2015/16 El Niño, especially in phase 4-5 and phase 7-8. It was clear that the RMM index was incapable of capturing the phenomenon that the MJO activity was weakened over the western Pacific and enhanced in the central and eastern Pacific during the mature phase of El Niño. However, this phenomenon could be reflected by the MJO amplitude (Figure 6). During the early mature stages of the 1982/83 and 1997/98 El Niño events, negative MJO amplitude anomalies mainly occurred in the Indian Ocean and western Pacific. With the evolution of time, the negative anomaly gradually expanded eastward, then extended to the central Pacific in the late mature stages and continued to the decaying stages (Figures 6A, B). The enhanced MJO amplitude primarily occurred in the central Pacific during the 1982/83 El Niño before December, while they were mainly appeared in the eastern Pacific after December (Figure 6A). In the 1997/98 El Niño, the MJO amplitude strengthened over the central and eastern Pacific before December, while prominent anomalies were not detected anymore over the central and eastern Pacific after December (Figure 6B). During the mature stages of the 2015/16 El Niño, negative MJO amplitude anomalies in the Indian Ocean and western Pacific were not obvious, but positive anomalies were significantly enhanced over the central and eastern Pacific, especially after November (Figure 6C).

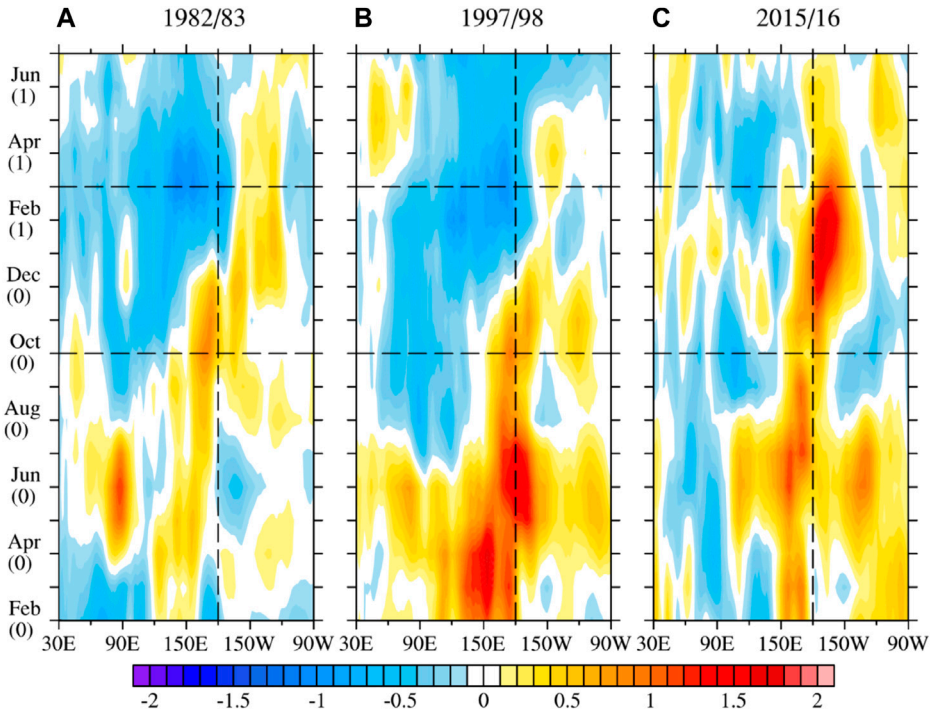

FIGURE 6
Anomalous MJO amplitude of zonal wind at 850 hPa averaged over 10°S—10°N during the three super El Niño events (m s^{-1}). The 0 and 1 represent super El Niño event onset and next year, respectively. **(A–C)** represent 1982/83,1997/98 and 2015/16, respectively.

3.3 Decaying stages

The eastward propagation of the MJO could be observed during the decaying stages of the three super El Niño, but their intensity, duration and propagation distance were significantly weakened compared with those in the developing and mature stages (Figure 2). The spatiotemporal spectral analysis in Figure 3 also showed that power spectrum of intraseasonal eastward propagation during the decaying stages of the 1997/98 and 2015/16 El Niño events were relatively stronger than those during the 1982/83 El Niño. The central periods of the eastward propagation for the MJO were mainly 40 days and 75 days during the decaying stages of 1997/98 El Niño, and it was primarily 40 days for the 2015/16 El Niño. However, there is no center of intraseasonal eastward propagation during the 1982/83 El Niño. The strong wave of eastward and westward propagation of lager than 90 days appeared in the decaying stages of the 1982/83 and 1997/98 El Niño events, which may be induced by the conversion of the MJO energy to low-frequency energy of above 90 days (Li and Zhou, 1994; Li and Li, 1995). At the same time, the high-frequency wave activities of the eastward propagation were prominent at 20–30 days during the decaying stages of the 1997/98 El Niño. In addition, the eastward propagation center of zonal wave 2 was detected during the decaying stages of the 1982/83 El Niño.

The evolution and composite results of the RMM index during decaying stages of three super El Niño illustrated that the MJO activity in the decaying stages is significantly weaker than that in the developing and mature stages. The MJO intensity in the decaying stages was the weakest, especially for the 1982/83 and 1997/98 El Niño events (Figure 2; Figure 4; Figure 5). The RMM indexes of phase 4–8 during the decaying stages of the 1997/98 and 2015/16 El Niño changed from positive anomaly in the mature stages to negative anomalies, particularly in phase 6–8 (Figure 5C). The strong MJO activity led to the increase in the average RMM index of phase 4-5 in May 1998. The two robust MJO activities in June and July 2016 also enhanced the average RMM index of phase 1-2 during the decaying stages of the 2015/16 El Niño. Many studies had indicated that the robust MJO activity in May 1998 triggered the easterly anomalies, resulting in the termination of El Niño. After the MJO event, the Niño 3.4 index rapidly decayed from positive anomaly to negative anomaly (Takayabu et al., 1999; Miyakawa et al., 2017). Figure 2 showed that during the decaying stages of three super El Niño, when Niño 3.4 index turned from positive to negative, the MJO easterly existed in the eastern Pacific, which demonstrated that the MJO easterlies may accelerate the extinction of strong El Niño. Meanwhile, the MJO westerlies in April 1998 and June 2016 existed in the eastern Pacific, while the decaying rate of the Niño 3.4 index was prominently reduced. The anomalous MJO zonal wind amplitudes in the Indian Ocean and Pacific were weakened in the decaying stages, especially in the 1982/83 and 1997/98 El Niño, while they were enhanced in the central and eastern Pacific, particularly in the 2015/16 (Figure 6). The MJO zonal wind amplitudes strengthened over the eastern Pacific, which may lead to the stronger 2015/16 El Niño. These results indicate that the MJO plays a critical role in the decaying stages of El Niño while it is

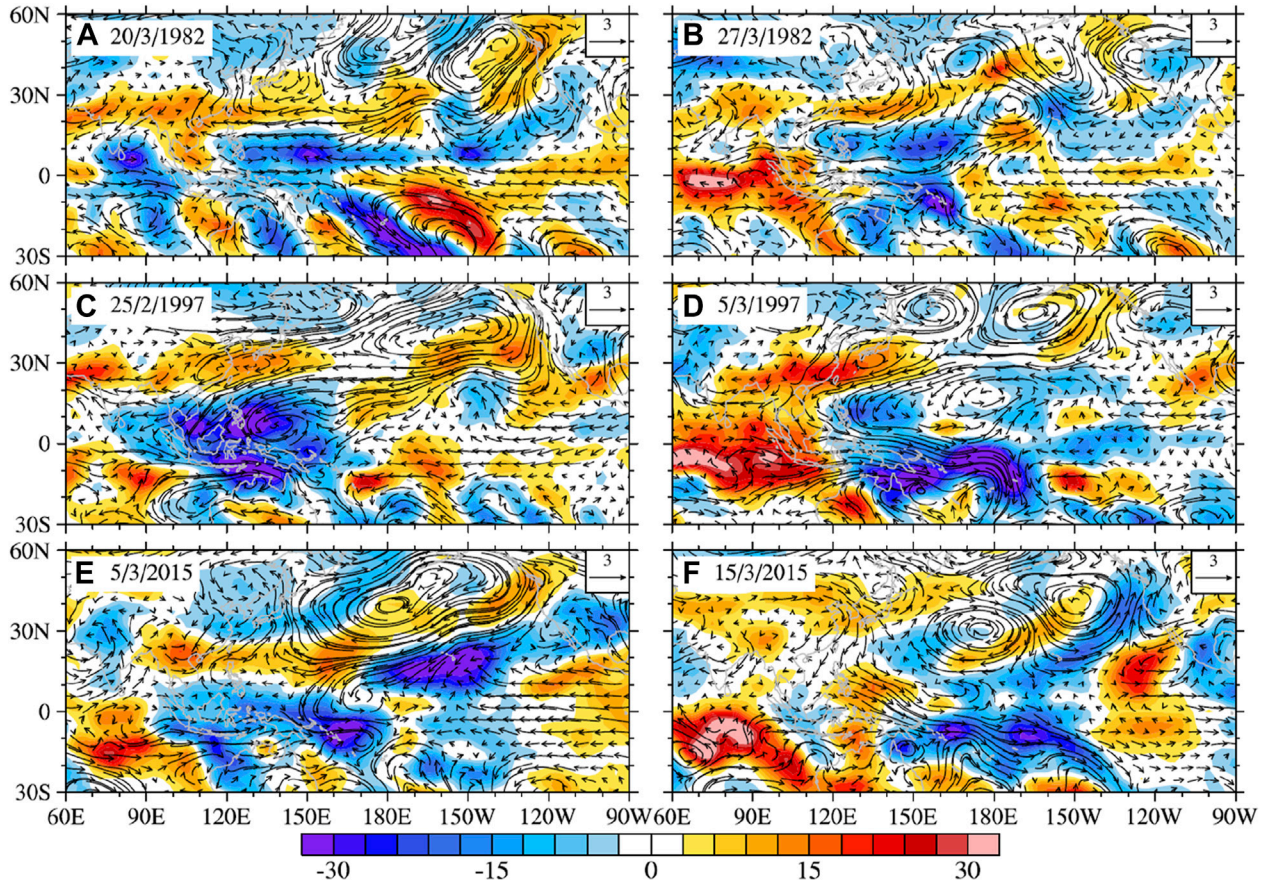

FIGURE 7
MJO wind at 850 hPa (vectors, m s^{-1}) and MJO OLR (colors, W m^{-2}) during the developing stages of the three super El Niño events. The 0 and 1 represent super El Niño event onset and next year, respectively. **(A–C)** represent 1982/83, 1997/98 and 2015/16, respectively.

necessary to further study the interaction between the MJO and the decaying stages of El Niño.

4 Possible cause of anomalous MJO activity

Figure 2 showed that the zonal westerlies of several MJO events were enhanced around 150°E during the early developing stages of three super El Niño, and the maximum center of MJO zonal wind occurred also around 150°E. Chen et al. (2017) indicated that the enhanced MJO zonal westerlies near 150°E are largely affected by the extratropical atmosphere. For the several MJO events during the developing stage of three super El Niño, our study discovered that the enhanced MJO zonal wind near 150°E is induced by extratropical circulation. Figure 7 shows the MJO circulation at 850 hPa and MJO OLR during the developing stage of the three super El Niño. The results clearly demonstrated that the MJO active near 150°E was closely related to the long-lasting extratropical circulations that reach the equator, which strengthened the activities of MJO zonal wind and OLR. The extratropical circulations originated from the northeastern Pacific (Figures 7A, C–E) as well as Siberia (Figures 7B, F). At the same time, due to the change of background field circulation (low-frequency circulation of more than 90 days) during the developing stages of El Niño, the MJO zonal westerly wind activity will strengthen around 150°E. From the anomalous 850 hPa zonal wind and specific humidity, it was clear that zonal westerly anomalies were appear in the western Pacific during the developing stages, and the strongest in the 1997/98 El Niño. The zonal winds of climate states over the central and eastern Pacific are robust easterlies and gradually weaken to the west. Thus, the anomalous westerly over the western Pacific amplify the zonal gradient of background zonal wind. Hsu et al. (2018) indicate that the conversion of low-frequency kinetic energy of more than 90 days to MJO kinetic energy is proportionate to the zonal gradient of background zonal wind ($-u'^2\frac{\partial \bar{u}}{\partial x}$, "′" and "–" are MJO scale and background wind). Therefore, the occurrence of background westerly anomaly over the western Pacific may lead to reinforcing the barotropic energy conversion from the low-frequency background field to the MJO scale, resulting in enhancing the activities of MJO zonal westerly.

In the mature stages of El Niño, the easterly anomaly from the Indian Ocean to the western Pacific Ocean, and the abnormal subsidence movement and negative moisture anomaly in the maritime continent and the western Pacific Ocean are not conducive to the MJO activities in these areas (Chen et al., 2016). The circulation and moisture anomaly in the western Pacific were relatively weak during the 2015/16 El Niño, so the weakening degree of MJO is relatively weak (Figure 8).

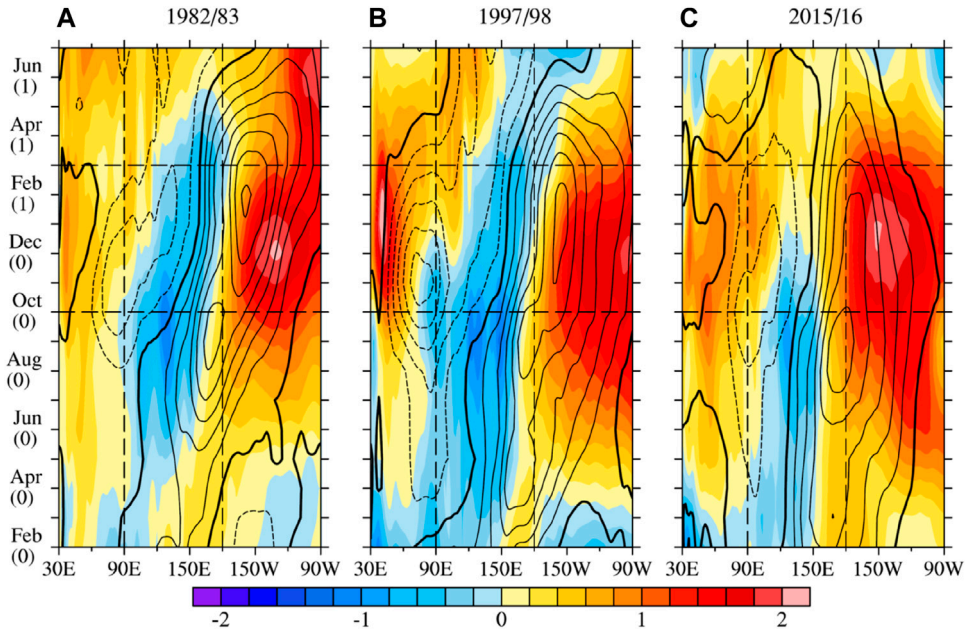

FIGURE 8
Anomalous zonal wind (contours, negative values are represented by dashed with the interval of 1 m s^{-1} and bold lines represent zero isolines) and specify humidity (colors, g kg^{-1}) at 850 hPa averaged over 10°S—10°N during the three super El Niño events. The 0 and 1 represent super El Niño event onset and next year, respectively. **(A–C)** represent 1982/83, 1997/98 and 2015/16, respectively.

Meanwhile, positive moisture anomaly and anomalous ascending motion appeared in the central and eastern Pacific during the mature stages of El Niño, which provide a favorable background field for the MJO activity, resulting in a stronger MJO amplitude over the central and eastern Pacific (Figure 6). It is noteworthy that the zonal westerly and positive moisture anomaly over the central and eastern Pacific was significantly westward during the mature stages of the 2015/16 El Niño, comparing with the other two El Niño events, which is consistent with the location of positive anomaly of MJO zonal wind amplitude to the west as shown in Figure 6. The circulation and moisture anomalies from the Indian Ocean to the western Pacific impeded the propagation of MJO during the mature stages of 1982/83 and 1997/1998 El Niño events, which caused the discontinuous eastward propagation. The 2015/16 El Niño showed some characteristics similar to the central Pacific El Niño (Paek et al., 2017). Although a certain easterly anomaly appeared over the western Pacific, the moisture was not prominent and positive moisture anomalies appeared in the later. Furthermore, the center of positive moisture anomaly over the central and eastern Pacific was westward. Consequently, the combination of anomalous moisture background and MJO circulation strengthens the moisture convergence in the lower troposphere on the eastern side of MJO convection ($-u'\frac{\partial \bar{q}}{\partial x}$), which promotes the activity and eastward propagation of MJO over the central and eastern Pacific (Chen et al., 2016).

In the decaying stages, the easterly anomaly and negative moisture anomaly over the western Pacific and maritime continent were also not conductive to the MJO activity in these areas. As the zonal westerly and positive moisture anomaly over the central and eastern Pacific rapidly weakened, resulting in weakening their strengthened role on the MJO. At the same time, the MJO activity weaken seasonally, due to the seasonal change of the background field (Dong et al., 2004). Therefore, the combination of anomalous circulation and moisture induced by El Niño with the seasonal variation of background field greatly weakened the MJO activity, which led to make the decaying stages the weakest period of MJO activity. However, the related physical process and mechanism of the abnormal MJO activity during the decaying stages of El Niño still need to be further researched.

5 Conclusion and discussion

The relationship between MJO and El Niño has always been a hot topic. Based on the reanalysis data, this paper deeply compared and analyzed the characteristics of MJO intensity and propagation during the developing, mature, and decaying stages of three super El Niño. Furthermore, this study identified the essential processes that induce abnormal MJO activities. The main conclusions are as follows:

There were three MJO events with obvious eastward propagation during the developing stages of the three super El Niño. The RMM index illustrated that MJO intensity decreased (or increased) in all phase during the developing stages of the 1982/83 (1997/98) El Niño event. The MJO activities weakened in phase 4–6 during the developing stages of the 2015/16 El Niño while significantly strengthened in other phases. In addition, the MJO zonal wind amplitude over the western Pacific strengthened during the developing stages of three super El Niño, especially during the 1997/98 El Niño.

The eastward propagation of MJO were not prominent during the mature stages of the 1982/83 and 1997/98 El Niño events, and there were even westward propagation. On the contrary, the prominent eastward propagation of MJO still appeared in the 2015/16 El Niño.

The RMM index showed that MJO intensities in all phase obviously decreased during the mature stages of the 1982/83 and 1997/98 El Niño events, while prominently increased in phase 4–8 during the 2015/16 El Niño. The MJO zonal wind amplitude weakened over the Indian Ocean and western Pacific during the mature stages of the 1982/83 and 1997/98 El Niño, while slightly strengthened over the central and eastern Pacific. However, MJO zonal wind prominently strengthened over the central and eastern Pacific during the mature stages of 2015/16 El Niño.

Although the eastward propagation of the MJO appeared during the decaying stages of three super El Niño, the intensity were weaker compared with the developing and mature stages, and decaying stages was the weakest stages of MJO activity. The RMM index indicated that the MJO primarily decreased in phase 1–3 and phase 6–8, while the MJO zonal wind amplitude mainly decreased over the Indian Ocean and western Pacific.

This study found that the activity and evolution characteristics of the MJO were mainly dominated by the low-frequency atmospheric circulation and anomalous moisture induced by El Niño, and they also were regulated by the extratropical circulation. In addition, the anomalous MJO activities played an obvious role in the developing and decaying stages of El Niño. This study also quantified the abnormal characteristics of MJO activities by the RMM index and MJO amplitude during the super El Niño, and there were contradictory results from the two method. Thus, we should pay more attention to they in the scientific research and practice applications to avoid misunderstanding the MJO characteristics. At present, many studies have focused on the interaction between MJO and El Niño during the developing and mature stages of El Niño. However, it is still necessary to further study the interaction between the MJO and El Niño during the decaying stages of El Niño and the corresponding cooperative effect on climate.

Data availability statement

The raw data supporting the conclusion of this article will be made available by the authors, without undue reservation.

Author contributions

XC provided the original idea and discuss with LL and CL. LL and XC plotted the figures and wrote the initial manuscript. XL and MY provided valuable advice for the research and presentation. All the authors contributed to the writing, editing, presentation, and reviewing of the manuscript.

Funding

This work was supported by the National Natural Science Foundation of China (Grant 42205045), the Hunan Natural Sciences Foundation (Grant 2022JJ30660), the National Key Research and Development Program of China (Grant 2018YFC1505901).

Acknowledgments

The ERA-Interim reanalysis dataset was obtained online (https://www.ecmwf.int/en/forecasts/datasets/reanalysis-datasets/era-interim). The Optimum Interpolation SST V2 (https://psl.noaa.gov/data/gridded/data.noaa.oisst.v2.html) and Extended Reconstructed SST V5 (https://psl.noaa.gov/data/gridded/) were provided by the NOAA. The MJO index was obtained from the Australian Bureau of Meteorology (http://www.bom.gov.au/climate/mjo/graphics/rmm.74toRealtime.txt).

Conflict of interest

The authors declare that the research was conducted in the absence of any commercial or financial relationships that could be construed as a potential conflict of interest.

Publisher's note

All claims expressed in this article are solely those of the authors and do not necessarily represent those of their affiliated organizations, or those of the publisher, the editors and the reviewers. Any product that may be evaluated in this article, or claim that may be made by its manufacturer, is not guaranteed or endorsed by the publisher.

References

Abellán, E., Mcgregor, S., England, M. H., and Santoso, A. (2018). Distinctive role of ocean advection anomalies in the development of the extreme 2015–16 El Niño. *Clim. Dyn.* 51, 2191–2208. doi:10.1007/s00382-017-4007-0

Bergman, J. W., Hendon, H. H., and Weickmann, K. M. (2001). Intraseasonal air–sea interactions at the onset of El Niño. *J. Clim.* 14, 1702–1719. doi:10.1175/1520-0442(2001)014<1702:iasiat>2.0.co;2

Bi, B., Zhang, X., and Dai, K. (2017). Characteristics of 2016 severe convective weather and extreme rainfalls under the background of super El Niño. *Chin. Sci. Bull.* 62, 928–937. doi:10.1360/n972016-01136

Chen, L., Li, T., Wang, B., and Wang, L. (2017). Formation mechanism for 2015/16 super El Niño. *Sci. Rep.* 7, 2975–3010. doi:10.1038/s41598-017-02926-3

Chen, X., Li, C., and Tan, Y. (2015). The influence of El Niño on MJO over the equatorial Pacific. *J. Ocean Univ. China* 14, 1–8. doi:10.1007/s11802-015-2381-y

Chen, X., Ling, J., and Li, C. (2016). Evolution of the madden–julian oscillation in two types of El Niño. *J. Clim.* 29, 1919–1934. doi:10.1175/jcli-d-15-0486.1

Dasgupta, P., Roxy, M., Chattopadhyay, R., Naidu, C., and Metya, A. (2021). Interannual variability of the frequency of MJO phases and its association with two types of ENSO. *Sci. Rep.* 11, 11541–11616. doi:10.1038/s41598-021-91060-2

Dee, D. P., Uppala, S. M., Simmons, A. J., Berrisford, P., Poli, P., Kobayashi, S., et al. (2011). The ERA-Interim reanalysis: Configuration and performance of the data assimilation system. *Q. J. R. meteorological Soc.* 137, 553–597. doi:10.1002/qj.828

Dong, M., Zhang, X., and He, J. (2004). A diagnostic study on the temporal and spatial characteristics of the tropical intraseasonal osicllation. *Acta Meteor Sin.* 62, 821–830. (in Chinese). doi:10.11676/qxxb2004.078

Duchon, C. E. (1979). Lanczos filtering in one and two dimensions. *J. Appl. Meteorology Climatol.* 18, 1016–1022. doi:10.1175/1520-0450(1979)018<1016:lfioat>2.0.co;2

Feng, J., Liu, P., Chen, W., and Wang, X. (2015). Contrasting madden–julian oscillation activity during various stages of EP and CP El niños. *Atmos. Sci. Lett.* 16, 32–37. doi:10.1002/asl2.516

Fink, A., and Speth, P. (1997). Some potential forcing mechanisms of the year-to-year variability of the tropical convection and its intraseasonal (25–70-day) variability. *Int.*

J. Climatol. A J. R. Meteorological Soc. 17, 1513–1534. doi:10.1002/(sici)1097-0088(19971130)17:14<1513::aid-joc210>3.0.co;2-u

Gushchina, D., and Dewitte, B. (2012). Intraseasonal tropical atmospheric variability associated with the two flavors of El Niño. *Mon. Weather Rev.* 140, 3669–3681. doi:10.1175/mwr-d-11-00267.1

Hayashi, Y. (1982). Space-time spectral analysis and its applications to atmospheric waves. *J. Meteorological Soc. Jpn. Ser. II* 60, 156–171. doi:10.2151/jmsj1965.60.1_156

Hendon, H. H., Wheeler, M. C., and Zhang, C. (2007). Seasonal dependence of the MJO–ENSO relationship. *J. Clim.* 20, 531–543. doi:10.1175/jcli4003.1

Hong, C.-C., Hsu, H.-H., Tseng, W.-L., Lee, M.-Y., Chow, C.-H., and Jiang, L.-C. (2017). Extratropical forcing triggered the 2015 madden–julian oscillation–el Niño event. *Sci. Rep.* 7, 46692–46698. doi:10.1038/srep46692

Hsu, P.-C., Fu, Z., and Xiao, T. (2018). Energetic processes regulating the strength of MJO circulation over the Maritime Continent during two types of El Niño. *Atmos. Ocean. Sci. Lett.* 11, 112–119. doi:10.1080/16742834.2018.1399049

Huang, B., Thorne, P. W., Banzon, V. F., Boyer, T., Chepurin, G., Lawrimore, J. H., et al. (2017). Extended reconstructed sea surface temperature, version 5 (ERSSTv5): Upgrades, validations, and intercomparisons. *J. Clim.* 30, 8179–8205. doi:10.1175/jcli-d-16-0836.1

Kessler, W. S., McPhaden, M. J., and Weickmann, K. M. (1995). Forcing of intraseasonal Kelvin waves in the equatorial Pacific *J. Geophys Res.* 100, 10613–10631.

Lau, K.-M., and Chan, P. H. (1988). Intraseasonal and interannual variations of tropical convection: A possible link between the 40–50 day oscillation and ENSO? *J. Atmos. Sci.* 45, 506–521. doi:10.1175/1520-0469(1988)045<0506:iaivot>2.0.co;2

Lau, K., and Chan, P. (1986). The 40–50 day oscillation and the El niño/southern oscillation: A new perspective. *Bull. Am. Meteorological Soc.* 67, 533–534. doi:10.1175/1520-0477(1986)067<0533:tdoate>2.0.co;2

Lee, R. W., Woolnough, S. J., Charlton-Perez, A. J., and Vitart, F. (2019). ENSO modulation of MJO teleconnections to the north atlantic and europe. *Geophys. Res. Lett.* 46, 13535–13545. doi:10.1029/2019gl084683

L'heureux, M. L., Takahashi, K., Watkins, A. B., Barnston, A. G., Becker, E. J., Di Liberto, T. E., et al. (2017). Observing and predicting the 2015/16 El Niño. *Bull. Am. Meteorological Soc.* 98, 1363–1382. doi:10.1175/bams-d-16-0009.1

Li, C., and Li, G. (1995). Kinetic energy changes in the tropical atmospheric system associated with El Niño. *Chin. Sci. Bull.* 40, 1866–1869. doi:10.1360/csb1995-40-20-1866

Li, C., Ling, J., Song, J., Pan, J., Tian, H., and Chen, X. (2014). Research progress in China on the tropical atmospheric intraseasonal oscillation. *J. Meteorological Res.* 28, 671–692. doi:10.1007/s13351-014-4015-5

Li, C., and Smith, I. (1995). Numerical simulation of the tropical intraseasonal oscillation and the effect of warm SST. *Acta Meteor. Sin.* 9, 1–12.

Li, C. (1995). Some fundamental problems of intraseasonal oscillation in the tropical atmosphere. *J. Trop. Meteorology* 11, 276–288. (in Chinese).

Li, C., and Zhou, Y. (1994). Relationship between intraseasonal oscillation in the tropical atmosphere and ENSO. *Chin. J. Geophys.* 37, 17–26. (in Chinese).

Li, Q., and Min, Q. (2016). A dialogue with Renhe Zhang: The heavy rainfall over southern China in the first half year of 2016 and its relation to the 2015/2016 super El Niño. *Chin. Sci. Bull.* 61, 2659–2662. doi:10.1360/zk2016-61-24-2659

Li, T., Ling, J., and Hsu, P.-C. (2020). Madden-Julian oscillation: Its discovery, dynamics, and impact on East Asia. *J. Meteorological Res.* 34, 20–42. doi:10.1360/zk2016-61-24-2659

Liu, M., Ren, H., Zhang, W., Ren, P., and Liu, X. (2018). An echo state network algorithm based on recursive least square for electrocardiogram denoising. *Acta Meteorol. Sin.* 76, 539–549. doi:10.7507/1001-5515.201710072

Lyu, Y., Li, Y., Tang, X., Wang, F., and Wang, J. (2018). Contrasting intraseasonal variations of the equatorial Pacific Ocean between the 1997–1998 and 2015–2016 El Niño events. *Geophys. Res. Lett.* 45, 9748–9756. doi:10.1029/2018gl078915

Madden, R. A., and Julian, P. R. (1972). Description of global-scale circulation cells in the tropics with a 40–50 day period. *J. Atmos. Sci.* 29, 1109–1123. doi:10.1175/1520-0469(1972)029<1109:dogscc>2.0.co;2

Madden, R. A., and Julian, P. R. (1971). Detection of a 40–50 day oscillation in the zonal wind in the tropical Pacific. *J. Atmos. Sci.* 28, 702–708. doi:10.1175/1520-0469(1971)028<0702:doadoi>2.0.co;2

Mcphaden, M. J. (1999). Genesis and evolution of the 1997-98 El Niño. *Science* 283, 950–954. doi:10.1126/science.283.5404.950

Mcphaden, M. J., Zhang, X., Hendon, H. H., and Wheeler, M. C. (2006). Large scale dynamics and MJO forcing of ENSO variability. *Geophys. Res. Lett.* 33, L16702. doi:10.1029/2006gl026786

Miyakawa, T., Yashiro, H., Suzuki, T., Tatebe, H., and Satoh, M. (2017). A Madden-Julian Oscillation event remotely accelerates ocean upwelling to abruptly terminate the 1997/1998 super El Niño. *Geophys. Res. Lett.* 44, 9489–9495. doi:10.1002/2017gl074683

Moon, J.-Y., Wang, B., and Ha, K.-J. (2011). ENSO regulation of MJO teleconnection. *Clim. Dyn.* 37, 1133–1149. doi:10.1007/s00382-010-0902-3

Mu, M., and Ren, H.-L. (2017). Enlightenments from researches and predictions of 2014-2016 super El Niño event. *Sci. China. Earth Sci.* 60, 1569–1571. doi:10.1007/s11430-017-9094-5

Paek, H., Yu, J. Y., and Qian, C. (2017). Why were the 2015/2016 and 1997/1998 extreme El Niños different? *Geophys. Res. Lett.* 44, 1848–1856. doi:10.1002/2016gl071515

Qian, D., and Guan, Z. (2018). Different features of super and regular El Niño events and their impacts on the variation of the West Pacific subtropical high. *Acta Meteorol. Sin.*, 394–407. doi:10.11676/qxxb2018.011

Rao, J., and Ren, R. (2017). Parallel comparison of the 1982/83, 1997/98 and 2015/16 super El Niños and their effects on the extratropical stratosphere. *Adv. Atmos. Sci.* 34, 1121–1133. doi:10.1007/s00376-017-6260-x

Ren, H.-L., Wang, R., Zhai, P., Ding, Y., and Lu, B. (2017). Upper-ocean dynamical features and prediction of the super El Niño in 2015/16: A comparison with the cases in 1982/83 and 1997/98. *J. Meteorological Res.* 31, 278–294. doi:10.1007/s13351-017-6194-3

Reynolds, R. W., Smith, T. M., Liu, C., Chelton, D. B., Casey, K. S., and Schlax, M. G. (2007). Daily high-resolution-blended analyses for sea surface temperature. *J. Clim.* 20, 5473–5496. doi:10.1175/2007jcli1824.1

Seo, K. H., and Xue, Y. (2005). MJO-related oceanic Kelvin waves and the ENSO cycle: A study with the NCEP Global Ocean Data Assimilation System. *Geophys. Res. Lett.* 32, L07712. doi:10.1029/2005GL022511

Shao, X., and Zhou, B. (2016). Monitoring and diagnosis of the 2015/2016 super El Niño event. *Meteorol. Mon.* 42, 540–547. (in Chinese). doi:10.7519/j.issn.1000-0526.2016.05.003

Takayabu, Y., Iguchi, T., Kachi, M., Shibata, A., and Kanzawa, H. (1999). Abrupt termination of the 1997–98 El Niño in response to a madden–julian oscillation. *Nature* 402, 279–282. doi:10.1038/46254

Tam, C.-Y., and Lau, N.-C. (2005). Modulation of the madden-julian oscillation by ENSO: Inferences from observations and GCM simulations. *J. Meteorological Soc. Jpn. Ser. II* 83, 727–743. doi:10.2151/jmsj.83.727

Vecchi, G., and Harrison, D. E. (2000). Tropical Pacific sea surface temperature anomalies, El Niño and equatorial westerly wind events. *J. Clim.* 13, 1814–1830. doi:10.1175/1520-0442(2000)013<1814:TPSSTA>2.0.CO;2

Wang, L., Li, T., Chen, L., Behera, S. K., and Nasuno, T. (2018). Modulation of the MJO intensity over the equatorial Western Pacific by two types of El Niño. *Clim. Dyn.* 51, 687–700. doi:10.1007/s00382-017-3949-6

Wei, Y., and Ren, H.-L. (2019). Modulation of ENSO on fast and slow MJO modes during boreal winter. *J. Clim.* 32, 7483–7506. doi:10.1175/jcli-d-19-0013.1

Wheeler, M. C., and Hendon, H. H. (2004). An all-season real-time multivariate MJO index: Development of an index for monitoring and prediction. *Mon. weather Rev.* 132, 1917–1932. doi:10.1175/1520-0493(2004)132<1917:aarmmi>2.0.co;2

Yuan, Y., Gao, H., Jia, X., and Wan, J. (2016). Influences of the 2014-2016 super El Niño event on climate. *Meteorol. Mon.* 42, 532–539. (in Chinese). doi:10.7519/j.issn.1000-0526.2016.05.002

Yuan, Y., Li, C., and Ling, J. (2015). Different MJO activities between EP El Niño and CP El Niño. *Sci. China Earth Sci.* 45, 318–334. (in Chinese). doi:10.1360/zd-2015-45-3-318

Zhai, P., Yu, R., Guo, Y., Li, Q., Ren, X., Wang, Y., et al. (2016). The strong El Niño in 2015/2016 and its dominant impacts on global and China's climate. *Acta Meteor Sin.* 74, 309–321. (in Chinese). doi:10.11676/qxxb2016.049

Zhang, C., and Gottschalck, J. (2002). SST anomalies of ENSO and the Madden–Julian oscillation in the equatorial Pacific. *J. Clim.* 15, 2429–2445. doi:10.1175/1520-0442(2002)015

Zhang, C. (2013). Madden–Julian oscillation: Bridging weather and climate. *Bull. Am. Meteorological Soc.* 94, 1849–1870. doi:10.1175/bams-d-12-00026.1

Zheng, Y., Chen, Z., Wang, H., and Du, Y. (2019). Features of 2015/2016 extreme El Niño event and its evolution mechanisms. *J. Trop. Oceanogr.* 38, 10–19. (in Chinese). doi:10.11978/2018114